

Chase-Escape Percolation on the 2D Square Lattice

Aanjaneya Kumar* and Deepak Dhar†

Department of Physics, Indian Institute of Science Education and Research, Dr. Homi Bhabha Road, Pune 411008, India

(Dated: October 13, 2020)

We study the chase-escape percolation model on the 2-D square lattice. In this model, prey particles spread to neighbouring empty sites at rate p , and predator particles spread only to neighbouring sites occupied by prey particles at rate 1, killing the prey particle that existed at that site. It is found that the prey can survive with non-zero probability, if $p > p_c$ with $p_c < 1$. Using Monte Carlo simulations, we estimate the value of p_c to be 0.4943 ± 0.0005 and the critical exponent for the divergence of the correlation length ν to be consistent with the 2D undirected percolation value $4/3$. We further show Chase-Escape percolation cannot fully be in the 2D undirected percolation universality class as for $p < p_c$ on a D -dimensional hypercubical lattice, the probability that the number of predators in the absorbing configuration is greater than s is bounded from below by $\exp(-Kp^{-1}s^{1/d})$, where K is some p -independent constant, in contrast to the exponentially decaying cluster size distribution of the isotropic percolation problem. We then study the problem starting from an initial condition with predator particles on all lattice points of the line $y = 0$ and prey particles on the line $y = 1$. In this case, for $p_c < p < 1$, the center of mass of the prey and predator fronts travel at the same speed and the two fronts fluctuate, but remain close to each other. We find that the speed of the pinned Chase-Escape front is strictly smaller than the speed of the Eden front when its spreading rate is equal to p and show that it is caused by the prey sites at the leading edge being eaten up by the predator. For $p > 1$, the prey front moves with a faster velocity to the right than the predator front. We study the depinning transition between the two fronts in the model at $p = 1$. At the depinning point, on a line of length L , the variance of the width of red front increases as $L^\alpha f(t/L^z)$, where f a scaling function, $\alpha \approx 1$, and $z = 1.67 \pm 0.1$.

I. INTRODUCTION

Growth and spreading processes are ubiquitous, e.g. growing crystals from supersaturated solutions [1, 2], dielectric breakdown [3, 4], bacterial colonies [5], growth of tumors [6, 7] and spreading of rumours in social networks [8–10]. Spreading processes and stochastic growth models have attracted a lot of attention in statistical physics, owing to their wide applicability and their beauty [11–14]. Simple mathematical models of these have provided us with much insight about their universal critical behavior, and more generally into nonequilibrium phenomena [15–18]. One of the earliest of such models was the Eden model of the tumour growth [12]. Many questions about this model have been studied, such as the velocity of its growth in different directions, the asymptotic shape, and fluctuations of the interface [14, 19]. Several variants have been studied, starting from the model of skin cancer by Williams and Bjerknes [20] to the SIR (Susceptible-Infected-Recovered) and SIS (Susceptible-Infected-Susceptible) models of epidemics [21]. The importance of such modelling has been underscored during the current COVID-19 pandemic, where specialized SIR-type models have been extensively used to better understand the course of the pandemic, and study the effects of different intervention strategies [22].

An important issue in Ecology and conservation studies is understanding how much predation would result

in prey population becoming extinct. Similarly, on social networks, one would like to know how efficient the rumour-scotching process has to be, to stop the spread of misinformation and rumours [8]. A simple model of this phenomena, called the *Chase-Escape* percolation was introduced recently, where it was shown that indeed a slowly growing prey populations can coexist with relatively fast growing predators. This is the subject of this paper. This model was first studied in [23] as a prey-predator model on trees where the prey tries to escape predators that are chasing it. Later, it was extended to lattices and graphs with cycles where the model displays very rich features [25, 27]. It was shown in Ref. [25] that Chase-Escape on the 2D square lattice undergoes a survival-extinction phase transition for the prey, and interestingly, the critical point for this phase transition was shown to be very close to $1/2$ [25], the well-known critical threshold of bond percolation on the square lattice [26]. In [27], $p_c = 0.5$ was called the conjectured critical value for Chase-Escape percolation on the square lattice.

While there is no real argument in favor of the critical value for Chase-Escape percolation on the square lattice being exactly $1/2$, it suggests a subtle connection to the ordinary bond percolation problem. One of the aims of our study was to determine the critical threshold in this model more precisely numerically by simulations. We find $p_c = 0.4943 \pm 0.0005$, which indicates that such a connection is unlikely. A finite size scaling analysis of the data gives value of the correlation length exponent ν close to the undirected 2D percolation value $4/3$, but we show that the model is not fully in the same universality class as undirected percolation, as the subcritical phase has a stretched exponential decay of the cluster size dis-

* kumar.aanjaneya@students.iiserpune.ac.in

† deepak@iiserpune.ac.in

tribution. We find that in the range $p_c < p < 1$, the common velocity of the prey front is less than what it would be in the absence of prey. This is different from the behavior found in some continuum predator-prey evolution models [28]. We explain the difference in terms of the discrete nature of the front, which is not well-captured in the continuum description. Finally, we study the depinning transition between the predator and prey fronts at $p = 1$, and estimate the corresponding roughness and dynamical exponents to be $\alpha \approx 1/2$, $z = 1.67 \pm .1$.

The plan of the paper is as follows: in the next section, we define the model precisely, and review earlier results. In section III, we discuss our Monte Carlo simulation procedure, and analysis, to estimate the critical value p_c . Finite size scaling analysis for different lattice sizes is used to determine the critical exponent ν corresponding to the divergence of correlation length away from p_c . In Section IV, we discuss, for the general D -dimensional Chase-Escape percolation, the subcritical regime with $p < p_c$, where all the prey particles eventually die out and the system enters one of its many absorbing states. We argue that the probability that the number of predators in the absorbing configuration is greater than s is bounded from below by $\exp(-Kp^{-1}s^{1/d})$, where K is some p -independent constant, in contrast to the usual percolation problem, where such distributions decay exponentially with s , for large s . In section V, we study if the critical threshold is direction dependent, as is known to happen in the well-studied case of directed percolation. We present evidence that it is not. Section VI is devoted to the second phase transition in this model, which is like a pinning-depinning transition of the predator and prey fronts, and occurs at $p = 1$, but has not been discussed much earlier. For $p < 1$, the prey and predator fronts move together at the same velocity. Our simulations show that this pinned Chase-Escape front travels slower than the Eden front moving at the same rate p . We discuss the difference from the results of Owen and Lewis for some continuum descriptions of prey-predator models [28]. We identify the mechanism for the slowing down of the prey front, and verify it using numerical simulations. We use finite-size scaling to estimate the dynamical exponent z and the roughness exponent for the front. In Section VII, we summarize our results and discuss some directions for further work.

II. DEFINITION OF THE MODEL

Chase-Escape percolation on D -dimensional hypercubical lattices is defined as follows: each site can either be occupied by a predator species particle (denoted by blue color), a prey species particle (denoted by red color) or it can remain vacant. At time $t = 0$, origin O is occupied by a blue particle. All the neighbour of the origin, are occupied by a red particle and all other sites are vacant. The evolution is a continuous time Markov process in which a red particle can give birth to another red par-

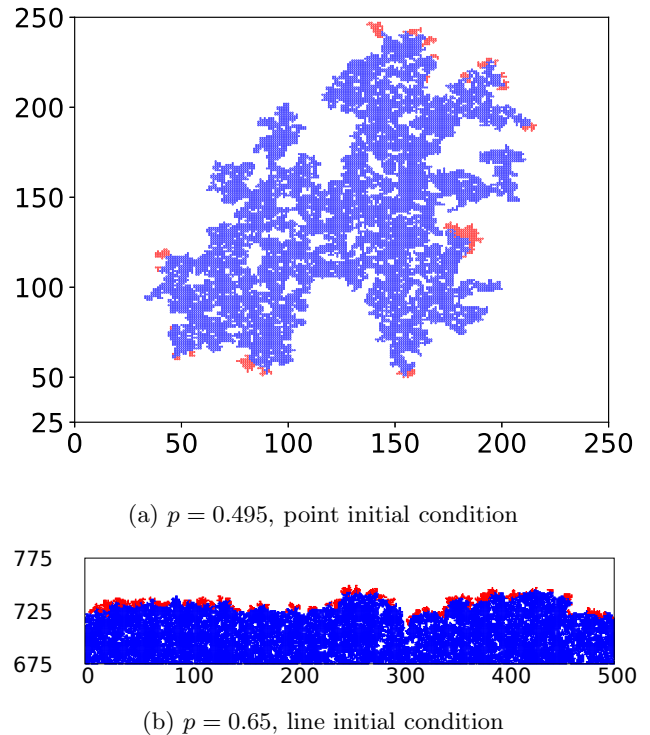


FIG. 1: Snapshots of realizations of the Chase-Escape process with different initial conditions: (a) for $p = 0.495$ on a 250×250 square lattice with a point initial condition (b) for $p = 0.65$ with a line initial condition on a lattice of size 500×1000 at time $t = 500$. For representation purposes, we restrict the range of y axis to present values between $y = 675$ to 775 for a close-up view of the *front*.

ticle at a vacant neighbouring site at rate p , and a blue particle can eat up a red particle at a neighbouring site at rate 1. When a predator eats up a prey particle on a neighbouring site, it gives birth to a predator at the site earlier occupied by the eaten prey. Note that the preys (the reds) can only reproduce at neighbouring vacant sites, and predators (the blues) reproduce only on eating a prey at a nearest neighbour site. If all the prey particles are eaten up, the predators cannot grow, and they do not die, so the the system goes into one of its many absorbing states.

In Fig. 1, we show the result of a typical evolution in the Chase-Escape model, starting from a point initial condition, and starting from a line initial condition (defined below).

This model has been studied on k -ary trees with initial conditions such that the predator is located at the root and the prey occupy the k daughters of the root [23, 24]. It was shown that the critical value for coexistence in this case is given by

$$p_c(k) = 2k - 1 - 2\sqrt{k^2 - k}. \quad (1)$$

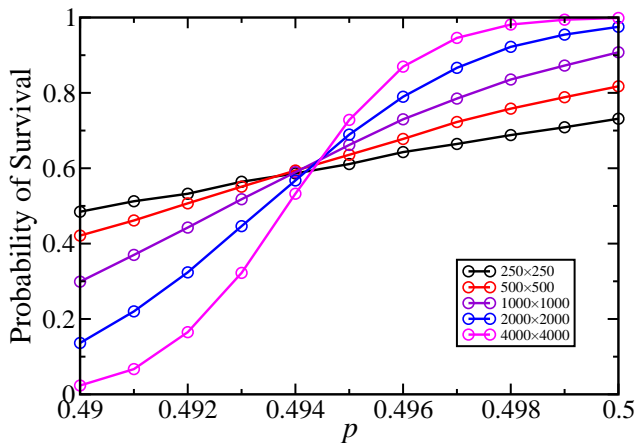


FIG. 2: Survival probability as a function of p is plotted for lattice sizes $L = 250, 500, 1000$ and 2000 . Observe the confluence of curves away from $p = 0.5$. The critical probability is determined to be 0.4943 ± 0.0005

Note that in large k limit, this gives $p_c \sim \frac{1}{4k}$. Clearly, it is seen that the prey can survive on such trees even if it moves at a slower rate than the predators and that the critical value p_c goes down as k increases. The Chase-Escape model was also studied on the ladder graph and it was found that its critical value is 1 [27].

The Chase-Escape model shows rich behaviour on $2D$ lattices and it was numerically explored in Ref. [25]. They showed convincingly that even on the square lattice, coexistence between the prey and predator is possible when the rate of spreading of prey p is strictly less than that of the predator. This is expected as the average number of vacant neighbors per prey particle is greater than the corresponding number of prey neighbors of a predator. As already mentioned, these authors noted that in this case, p_c is very close to $1/2$.

III. IMPROVED DETERMINATION OF CRITICAL PROBABILITY p_c

We used Monte Carlo simulations to determine more precisely the critical value p_c on the square lattice. We simulated the process on an $L \times L$ lattice with periodic boundary conditions along the x -axis and initial conditions such that each site on the line $y = 0$ is occupied by a predator particle and each site on the line $y = 1$ is occupied by a prey particle. With this ‘line’ initial condition, the boundaries of the clusters are statistically stationary for translations along the x -direction, and there is greater self-averaging in the evolving clusters, and the transition becomes much sharper than the initial condition where we start with a single predator. Throughout this work, we will work the line initial conditions, unless explicitly stated otherwise.

In a simulation on a $L \times L$ lattice, we say that the prey survives if any of the prey particles are able to reach

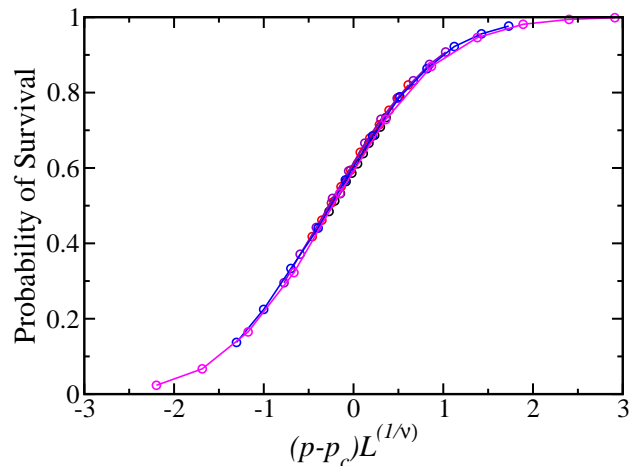


FIG. 3: Scaling collapse for the survival probability is plotted against $(p - p_c)L^{1/\nu}$, with $\nu = 1.33$ and $p_c = 0.4943$.

the line $y = L$ starting from the line initial condition. Survival probability is then calculated by performing the simulation multiple times and computing the fraction of realizations in which the prey survives. We used 50000 realizations to estimate the survival probability for each value of p and L . The plot of survival probability as function of p , for $L = 250, 500, 1000, 2000$ and 4000 is shown in Fig. 2.

We see that the curves for different L seem to meet at a common point at $p \approx 0.4943$. From the finite-size scaling theory, this point is identified as the critical probability. From the spread of the region of intersection, we estimate the error bar in this estimate to be 0.0005. We thus get estimate for the critical probability to be $p_c = 0.4943 \pm 0.0005$. Thus, our simulations strongly suggest that p_c is strictly less than $\frac{1}{2}$.

In Figure 3, we show the results of a finite-size scaling analysis of the data. We plot the survival probability against $(p - p_c)L^{1/\nu}$, and obtain a good data collapse for the values $p_c = 0.4943$ and $\nu = 1.33 \pm 0.01$. The numerical estimate of ν is in good agreement with its value in the standard $2D$ percolation universality class.

Chase-Escape percolation is somewhat similar to the SIR model, which belongs to the same universality class as the undirected percolation [31]. In the SIR model, each site is either Susceptible, Infected or Recovered. Infected sites can infect neighbouring sites that are susceptible and each infected site can recover independently. In some variants of this process, recovered sites become susceptible again with added immunity. In Chase-Escape percolation, the vacant sites can be thought of as susceptible, sites occupied by prey particles as infected and the ones occupied by predators as recovered. The key difference between the two models however is that in the SIR process, the recovery of each infected particle is independent of others whereas in Chase-Escape, the recovery can occur only at a site neighboring a recovered site, and the

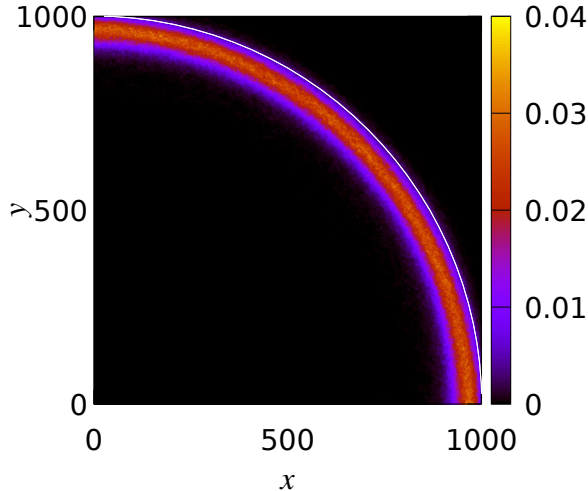


FIG. 4: $P(x, y|p)$ for $p = 0.6$ on a 2000×2000 square lattice. A circle (white) of radius 1000 is drawn for comparing the departure of the Chase-Escape cluster from the Euclidean ball.

predators always form a single connected cluster.

IV. LOWER BOUND TO THE CLUSTER SIZE IN THE ABSORBING STATE

In Section III, we showed that our estimate of critical exponent ν is same as for ordinary undirected percolation in two dimensions. One may then expect that the Chase-Escape transition is in the universality class of undirected percolation. However, this cannot be fully correct.

Consider the Chase-Escape percolation on the D -dimensional hypercubical lattice starting from the initial condition that the origin O is occupied by a prey and a predator is present at a neighboring site Q . We consider the case $p < p_c$, when the system eventually reaches one of its absorbing states and we are left with a cluster of predators.

Let $\text{CumProb}(s)$ denote be the probability that, in the absorbing state, the number of predators is greater than s . It is clear that this probability will be bounded from below by the probability that the prey population reaches s before the predator at site Q eats up its first prey. The probability that the predator at site Q does not eat its the adjacent prey up to time T is $\exp[-T]$, but in that much time, the number of prey particles grows to order of $(pT)^D$. It is clear that for the prey population to reach size s , the time required would be of order $s^{1/D}/p$. This immediately gives us

$$\text{CumProb}(s) \geq C_1 \exp \left[-\frac{C_2 s^{1/D}}{p} \right] \quad (2)$$

where C_1 and C_2 are constants, which may be chosen to independent of p . This is in contrast to ordinary percolation, where $\text{CumProb}(s)$ decreases exponentially with s ,

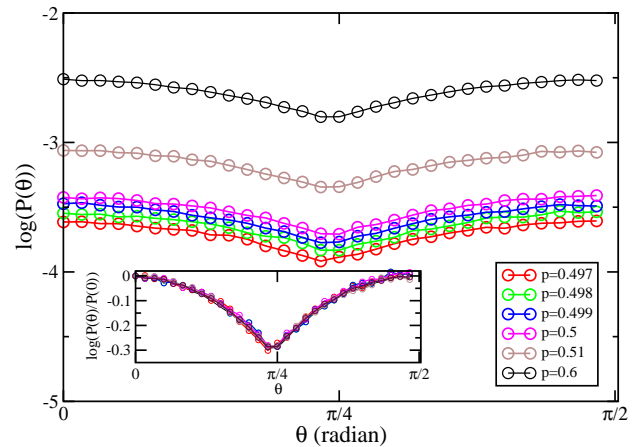


FIG. 5: $\log P(\theta|p)$ as a function of θ for different values of $p > p_c$. Inset shows a data collapse in the plot of $\log(P(\theta|p)/P(0|p))$ as a function of θ .

for large s for values below the critical threshold, follows an exponential decay.

In classifying critical phenomena, a universality class is characterized by all members of a class having the same set of critical exponents. In addition, the scaling functions near the critical point are also expected to be the same. In this stronger sense of universality, Chase-Escape percolation would not be in the universality class of undirected percolation, as the scaling function for the cluster size distribution would have to be different.

V. DIRECTION DEPENDENCE OF SURVIVAL PROBABILITY

The qualitative reason why the faster predators have front velocity same as the prey in the regime $p_c < p \leq 1$ is clearly due to the fact that the predators can only move along the sites occupied by the prey. But the paths created by the prey along different directions are qualitatively different. This can also be seen from the fact that front velocity of the prey in the Eden model, with no prey present is different in different directions. Simulations by Alm and Deijfen have shown that in $2D$, the velocity along the diagonal is smaller than the velocity along axis by roughly 1.3% [32]. It seems plausible that if the front velocity in different directions is different for the prey, even the critical thresholds could be different in different directions. We recall that in the well-studied case of directed percolation, there is a orientation dependence of the critical threshold $p_c(\theta)$, and infinite directed paths in the direction θ appear only if the probability $p > p_c(\theta)$.

To study the spatial distribution of the surviving prey look like, for $p > p_c$, we simulated the chase-escape process on the $2D$ square lattice starting from an initial condition where a single predator is present at the centre of the lattice, and all four of its neighbouring sites are occupied by prey particles. Each realization of this process is

run until all the prey die, or any of the prey reach any of the boundaries of the square lattice. At the end of each realization, we note the positions of the surviving prey. We define a spatial survival probability $P(x, y|p)$ which denotes the fraction of realizations in which a surviving prey was present at position (x, y) on the lattice. This allows us to define a direction dependent survival probability for a given p , $P(\theta|p)$, which equals the sum of survival probabilities $P(x, y|p)$ at the sites (x, y) , which satisfy $\tan^{-1}(y/x) \in [\theta - d\theta, \theta + d\theta]$.

In Fig. 4, we plot $P(x, y|p)$ for $p = 0.6$ for the first quadrant of a 2001×2001 square lattice. The probabilities in Fig. 4 are obtained by simulating the Chase-Escape process over 20000 realizations. We see that the average population of surviving prey is distributed in a roughly circular ring. The shape has the expected four-fold symmetry of the square lattice, but the calliper width along the diagonal is a few percent less than along the axes. For convenient comparison, we also plot in Fig. 4, a circle of radius 1000 which shows the departure of the Chase-Escape cluster from a Euclidean ball.

In Fig. 5, we plot $\log P(\theta|p)$ as a function of θ for different values of $p > p_c$ and show that the survival probability is maximum along the axis, and least along the diagonal. It is interesting to note that as soon as p becomes greater than p_c , $P(\theta|p)$ becomes non-zero for all θ . Change in the value of p seems to increase all $P(\theta|p)$ approximately by the same factor. Thus, to a good approximation, near p_c , we can write $P(\theta|p)$ as a product of two factors, one only depending on p , and one only on θ , i.e. $P(\theta|p) \approx Q(p)R(\theta)$. This is seen in the inset of Fig. 5, when $\log(P(\theta|p)/P(0|p))$ is plotted as a function of θ . We see that data for different p fall on same curve.

We also tried to determine p_c directly along the diagonal direction by using a line initial condition and studying the survival probability as function of p for different transverse sizes L . The results are shown in Fig. 6. We see that again the different curves seem to meet at a value $p_c = 0.494 \pm .001$, with a comparable quality of confluence, as compared with Fig. 2. Our simulations are not adequate to detect any direction dependence of p_c . If there is a difference, then it is small, of order 10^{-3} . More extensive simulations are needed to settle this question.

VI. DYNAMICS OF THE FRONTS FOR $p > p_c$

A picture of the interface for $p = 0.65$ was shown in Fig. 1(b). We can see that the red sites form a rather large number of disconnected clusters. The front does become smoother for larger p . In any case, for our discussion it is convenient to work with a single-valued height functions $h_{red}(x, t)$ and $h_{blue}(x, t)$, called the red and blue front heights respectively, at time t , that specifies the largest y -coordinate among all sites ever reached with that value of x -coordinate by that color up to time t . We will study here the mean values and variances of the

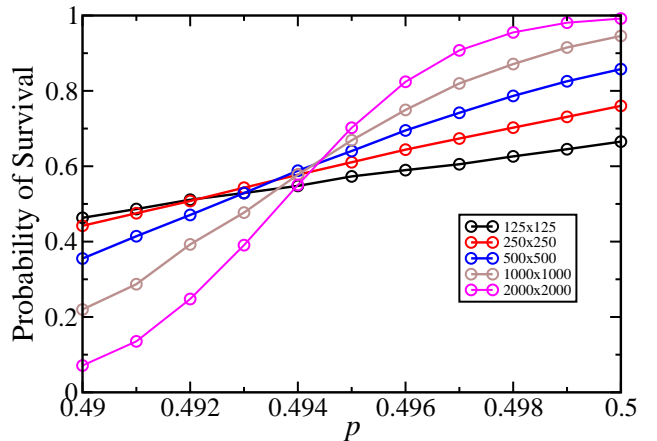


FIG. 6: The survival probability as a function of p for different transverse size L , with initial source along the

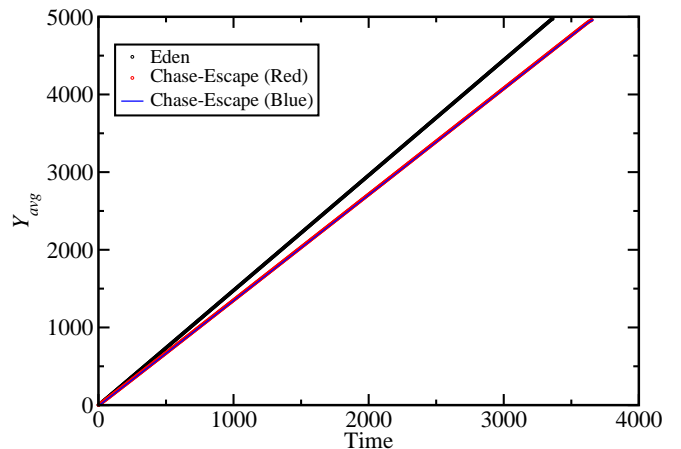


FIG. 7: Chase-Escape and Eden fronts at $p = 0.6$. It is easily seen that the centre of mass of prey and predator fronts coincide at all times showing that in the regime $p_c < p < 1$, the red and blue fronts are *pinned* together.

quantities, and their dependence on t . Note that if for some x , there is no red site at time t , then that particular value of x is disregarded during the computation of the height statistics. It is easy to see that for $p > 1$, the mean distance $w(t)$ between the prey and predator fronts increases linearly with time. For $p < p_c$, the system goes into one of its absorbing states and then $w(t)$ is exactly zero.

We studied the dynamics of the prey and predator fronts by numerical simulations on a lattice of dimensions 500×5000 with periodic boundary conditions along the x -axis, unless explicitly stated otherwise. For $p_c < p < 1$, we find that the centre of mass of the prey and predator fronts move together at the same velocity. In this regime, the two fronts are *pinned* together and at $p = 1$, a *depinning transition* [33, 34] occurs.

Figure 7 is a plot of the position of the centre of mass

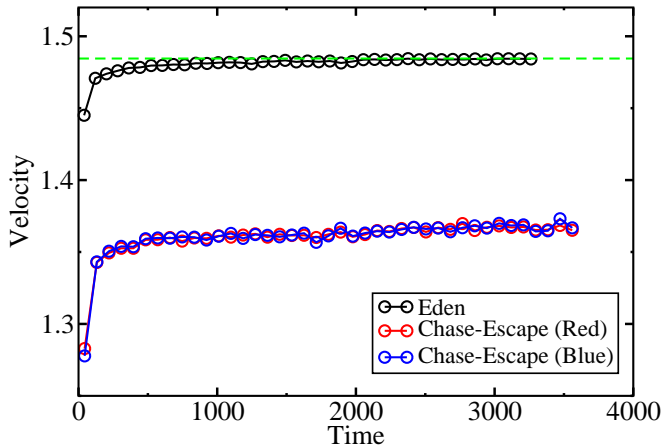


FIG. 8: Average velocities of the three fronts over a sliding window of 100 units as a function of time to check for convergence of velocity. The dashed green line depicts the Eden velocity from the simulations of Alm and Deijfen.

of prey and predator fronts at $p = 0.6$, as a function of time, averaged over 1000 realizations. We also show mean position of the Eden front, where each particle creates a copy of itself at an empty nearest neighbour site at rate 0.6. We clearly see that the prey and predator fronts travel at the same velocity, and that the Chase-Escape front on an average travels significantly slower than the Eden front moving at rate p . In Fig. 8, we plot the average velocities of the centre of mass of the prey and predator fronts, over a sliding window of size 100 units, at $p = 0.6$ and also of the Eden front travelling at the same speed. The dashed green line is the velocity of the Eden front as obtained by Alm and Deijfen. Our simulation of the Eden front is in agreement with their result. It is clear that the front velocity in Chase-Escape is strictly less than the what it would be if prey were absent.

This is somewhat surprising. It was shown by Owen and Lewis in a rather general continuum model of predator-prey dynamics that prey front velocity is unaffected by the presence of a predator, except if some special conditions are satisfied. The dynamics of Owen and Lewis model is described by the equations

$$\begin{aligned} \frac{\partial u}{\partial t} &= \epsilon D \frac{\partial^2 u}{\partial x^2} + ru f(u) - \phi v h(u) \\ \frac{\partial v}{\partial t} &= D \frac{\partial^2 v}{\partial x^2} + \gamma v h(u) - \delta v \end{aligned} \quad (3)$$

where u and v denote the population densities of prey and predators respectively and $f(u)$ and $h(u)$ are arbitrary positive functions [28].

Here $f(u)$ is a effective reproduction rate per individual. Usually, we expect $f(u)$ to be a decreasing function of u . However, sometimes, for very small u , the reproduction rate may decrease, say because of difficulty of finding a mate. If $\frac{df(u)}{du} > 0$ in some range of u , and an increase in density of prey leads to an increase in reproduction

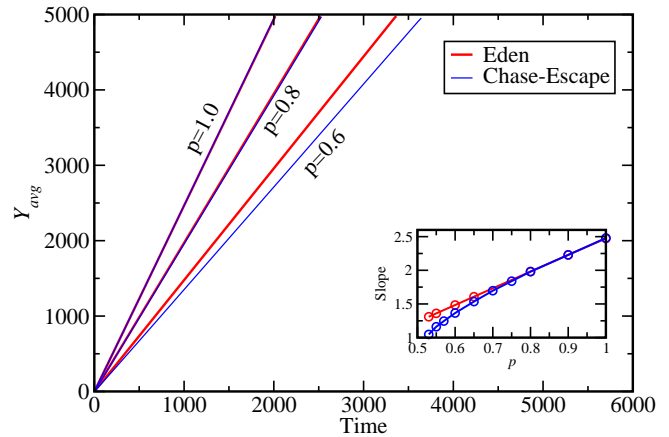


FIG. 9: Chase-escape (CE) and Eden fronts at values $p = 0.6, 0.8$ and 1. We can see that the Eden and CE fronts coincide at $p = 1$. As pointed in Figure 6, the CE front is significantly slower than the Eden front at $p = 0.5$. Inset is a plot of velocity of the CE and Eden fronts as a function of p . Clearly, velocity of the CE front in the pinned regime is not linear in p .

rate per individual, this is called the *Allee effect*. Owen and Lewis showed that, if the dynamics is described by Eq. 3, and there is no Allee effect, the velocity of prey front is not affected by the presence of predators. For the CE problem, increasing density of prey can not increase the reproductive rate, and there is no Allee effect. Hence, the surprise.

Figure 9 is a plot of Chase-Escape and Eden fronts at values $p = 0.6, 0.8$ and 1. We can see that the centre of mass of the Eden and Chase-Escape fronts coincide at $p = 1$, and move at the same velocity. However, at $p = 0.6$, the Chase-Escape front is significantly slower. The inset of Figure 9 further reveals that the velocity of the fronts in the pinned regime is not linear in p . What could be the reason for this discrepancy, and the inapplicability of the Owen and Lewis analysis for Chase-Escape percolation?

A clear difference between the Chase-Escape and Eden front is that the Chase-Escape front consists of inactive parts (sites occupied by predators) that can only grow if there is a prey adjacent to it. In the Chase-Escape front, it is also possible that the prey occupying the maximum position of the front, defined as the largest y -coordinate among all the surviving prey is eaten up by a predator, and the maximum of y -coordinate of red sites actually decreases. This contributes to the Chase-Escape front velocity becoming less than the Eden front velocity. Figure 10 provides evidence in favour of this argument where we plot the maximum y coordinate of the red particles (Y_{\max}) at $p = 0.6$ for Eden front and the prey front in Chase-Escape. Inset shows a zoomed in picture of the trajectory of the prey front where it is clearly visible that the maximum position of does drop quite often. Figure 11 shows four other instances from the trajectory of the

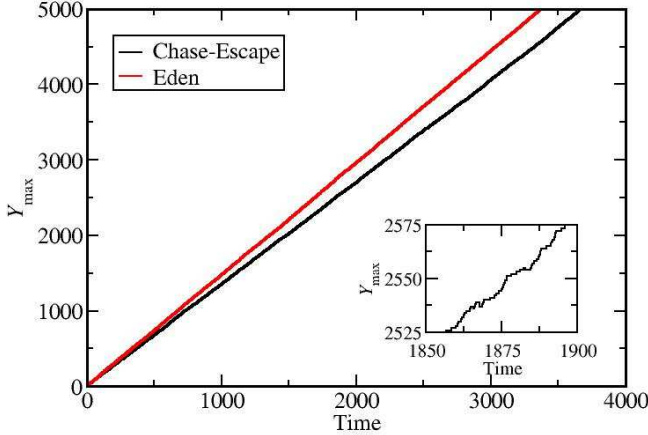


FIG. 10: Two trajectories of the maximum extent of infection at $p = 0.6$ for a single realization of the Eden front and the red front in CE are plotted. Inset shows a zoomed in picture of the trajectory of the CE front where it is clearly visible that the maximum position of

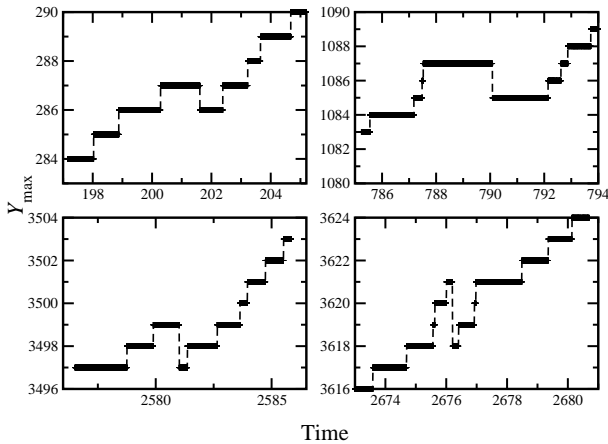


FIG. 11: Four instances from the trajectory in Fig. 10 where there is a drop in the maximum position of the red front.

maximum prey front where the drop is clearly visible. At $p = 0.6$, the backward motion occurs roughly 1% of the time on a lattice of size 500×5000 .

We believe that the reason for this is the discrete nature of the model, which is not correctly captured in the coarse-grained continuum equations of the type described in Eq. 3. In the coarse-grained continuum description, $u(x)$ has a rapidly decaying tail of the distribution for large x , but $u(x)$ is always non-zero at finite x , and there is no rightmost particle. But in the discrete model there is, and there is a non-zero probability that this gets eaten up by the predators. These events lead to an overall de-

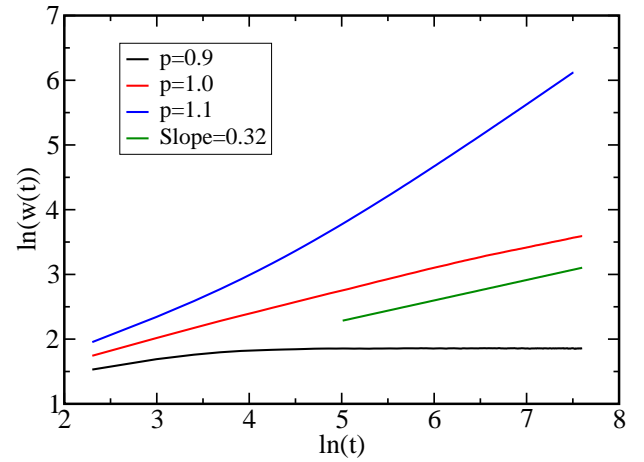


FIG. 12: Mean difference between the prey and predator fronts $w(t)$, for the values $p = 0.9, 1$ and 1.1 . At $p = 0.9$, the difference tends to a constant, and at $p = 1.1$, it grows linearly with time. At the critical point $p = 1$, $w(t)$ grows as $t^{0.32}$.

crease in the velocity of the prey front. Thus the discrete nature of the fluctuations of the front leads to a macroscopic observable consequence, which is not describable in the continuum description.

In Fig. 12, we plot the mean width $w(t)$ between the prey and predator fronts, as a function of time, for the values $p = 0.9, 1$ and 1.1 . As expected, at $p = 0.9$, the process is in the pinned regime and $w(t)$ tends to a finite constant. At $p = 1.1$, the mean width between the fronts grows linearly with time and is given by $w(t) = 0.24t$, and this is fully in line with the expectation that in this case, the blue front moves with the velocity of Eden front, and the red front velocity is 1.1 times the blue front velocity. However, at the critical point $p = 1$, by continuity arguments, one would expect that $w(t) \sim t^\zeta$ with $\zeta < 1$. This expectation is verified in our numerical simulations, and we observe that $w(t)$ shows a power law growth, with an exponent $\zeta = 0.32$. Furthermore, for both the regimes, $p > 1$ and $p < 1$, one would expect that the fluctuations in the Chase-Escape front are captured by KPZ theory, and the process falls in the KPZ universality class [15, 16].

We studied the fluctuations of the Chase-Escape front at the critical value $p = 1$. In Fig 13, we plot the scaled variance of the prey front as a function of time for lattice sizes $L \times 5000$, with L taking values 20, 40, 80, 160, 320 and 640. The left panel is a plot of the scaling of the variance by L^α , with $\alpha = 0.98$ which leads to a good data collapse for the asymptotic variance of the prey front. For the dynamical scaling, we ignore transient times of $t < 10$, and plot in the right panel, the scaled variance of the red front, as a function of scaled time where time has been scaled by a factor of L^z with $z = 1.67 \pm 0.1$. The exponents obtained at the critical point do not allow us to make conclusive remarks since $\alpha = 0.98$ is indis-

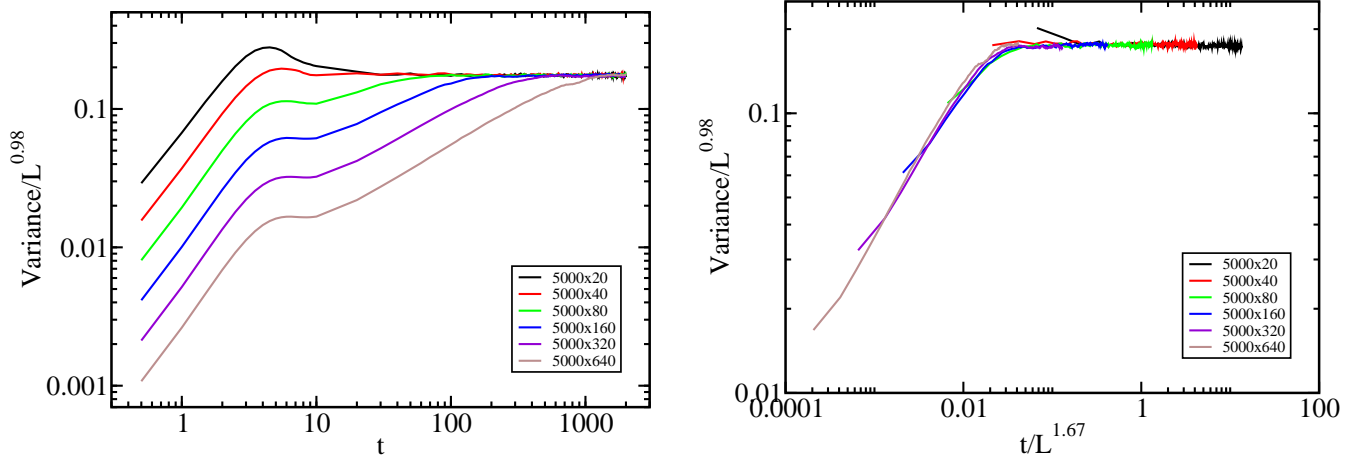


FIG. 13: Scaled variance as a function of time at $p = 1$. (Left) Scaling of the variance by L^α , with $\alpha = 0.98$ leads to a good data collapse for the asymptotic variance of the prey front. (Right) Scaling of time by L^z , with dynamical exponent $z = 1.67$, the data presented in the scaling plot does not include the transient time of $t < 10$.

tinguishable from the corresponding exponent from the KPZ universality class ($\alpha = 1$). The dynamical exponent of $z = 1.67$ however is significantly larger than value $3/2$, the dynamical exponent the KPZ universality class. Larger simulations are needed to determine this exponent more accurately.

VII. SUMMARY

In summary, we studied the Chase-Escape percolation on the $2 - D$ square lattice. We estimated the critical probability for the survival-extinction phase transition in this model from Monte Carlo simulations, and our final estimate is that $p_c = 0.4943 \pm 0.0005$ and we can thus say with fair confidence that $p_c \neq 1/2$. From the finite size scaling analysis near this transition, we find that the correlation length exponent ν is equal to the $2D$ undirected percolation value $4/3$ within our errorbars. We also point out that the subcritical phase of Chase-Escape percolation differs from the usual percolation problem, as in Chase-Escape, the cluster size distribution is not an exponentially-tailed distribution for any non-zero p .

For p just above p_c , we studied the direction dependence of the survival probabilities with the point initial condition, and showed that it seems to become non-zero along all directions, as soon as p is above p_c , and that this survival probability $P(\theta, p)$ along the direction θ at concentration p asymptotically tends to a factorized form $F(\theta)G(p)$, where $G(p)$ tends to zero, as p tends to p_c from above. Our simulations show that in the regime $p_c < p < 1$, the prey and predator fronts move with a common velocity, that is strictly less than than the velocity prey would have if predators were absent. We suggest

that this effect depends crucially on the discrete nature of fluctuations of the advancing front. Sometimes the leading prey on the front get eaten by predators, and this leads to temporary stoppage of advance of the local front.

There are several questions that still remain unanswered about Chase-Escape percolation. It would be nice to extend the results about the ladder to all graphs with a finite width, which are essentially one-dimensional, and prove that here p_c is always 1. Also, it would be nice to have a rigorous proof that for a regular d -dimensional lattice p_c for Chase-Escape percolation, p_c is strictly less than 1. More generally, determination of the exact front velocity or critical probability for some non-trivial non-tree graph is an open problem. The inclusion of a third species, that can only eat up the predators, could lead to non-trivial changes in the critical behaviour of the process, like the emergence of a multicritical point where all three fronts depin together. Moreover, if we allow for cyclic interactions where the prey, along with spreading on empty sites, can also eat up new species, many new and interesting features would emerge. These seem to be interesting directions for further study.

ACKNOWLEDGEMENTS

Aanjaneya Kumar would like to acknowledge the Prime Minister's Research Fellowship for financial support.

This paper is dedicated to the memory of Dietrich Stauffer, who was a friend, and collaborator of one of us. DD fondly remembers his wit and wisdom, dedication to physics, and ever helpful nature. It has been a privilege knowing him.

- [1] Nancollas, G.H., 1979. The growth of crystals in solution. *Advances in Colloid and Interface Science* 10, 215–252. [https://doi.org/10.1016/0001-8686\(79\)87007-4](https://doi.org/10.1016/0001-8686(79)87007-4)
- [2] Nielsen, A.E., 1969. Nucleation and Growth of Crystals at High Supersaturation. *Kristall und Technik* 4, 17–38. <https://doi.org/10.1002/crat.19690040105>
- [3] Li, X., Tung, C.H., Pey, K.L., 2008. The nature of dielectric breakdown. *Appl. Phys. Lett.* 93, 072903. <https://doi.org/10.1063/1.2974792>
- [4] Niemeyer, L., Pietronero, L., Wiesmann, H.J., 1984. Fractal Dimension of Dielectric Breakdown. *Phys. Rev. Lett.* 52, 1033–1036. <https://doi.org/10.1103/PhysRevLett.52.1033>
- [5] Allen, R.J., Waclaw, B., 2019. Bacterial growth: a statistical physicist’s guide. *Reports on Progress in Physics* 82, 016601. <https://doi.org/10.1088/1361-6633/aae546>
- [6] Waclaw, B., Bozic, I., Pittman, M.E., Hruban, R.H., Vogelstein, B., Nowak, M.A., 2015. A spatial model predicts that dispersal and cell turnover limit intratumour heterogeneity. *Nature* 525, 261–264. <https://doi.org/10.1038/nature14971>
- [7] Brú, A., Albertos, S., Luis Subiza, J., García-Asenjo, J.L., Brú, I., 2003. The Universal Dynamics of Tumor Growth. *Biophysical Journal* 85, 2948–2961. [https://doi.org/10.1016/S0006-3495\(03\)74715-8](https://doi.org/10.1016/S0006-3495(03)74715-8)
- [8] Nekovee, M., Moreno, Y., Bianconi, G., Marsili, M., 2007. Theory of rumour spreading in complex social networks. *Physica A: Statistical Mechanics and its Applications* 374, 457–470. <https://doi.org/10.1016/j.physa.2006.07.017>
- [9] C. O’Connor and J. O. Weatherall, *The Misinformation Age: How False Beliefs Spread* (Yale University Press, 2019).
- [10] LaCroix, T., Geil, A., and O’Connor, C. The dynamics of retraction in epistemic networks. Preprint. (2019)
- [11] J. M. Hammersley and D. J. A. Welsh, in *Bernoulli 1713 Bayes 1763 Laplace 1813: Anniversary Volume*, edited by J. Neyman and L. M. Le Cam (Springer Berlin Heidelberg, Berlin, Heidelberg, 1965), pp. 61–110.
- [12] Eden, M., 1961. A Two-dimensional Growth Process. In *Proceedings of the Fourth Berkeley Symposium on Mathematical Statistics and Probability*, edited by F. Neyman (Univ. of California Press, Berkeley, 1961), Vol.IV, p.233
- [13] Hammersley J.M., Welsh D.J.A., 1965. First-Passage Percolation, Subadditive Processes, Stochastic Networks, and Generalized Renewal Theory. In: Neyman J., Le Cam L.M. (eds) *Bernoulli 1713, Bayes 1763, Laplace 1813*. Springer, Berlin, Heidelberg. <https://doi.org/10.1007/978-3-642-49749-0>
- [14] Auffinger, A., Damron, M. and Hanson, J., 2017. 50 years of first-passage percolation (Univ. Lecture Series, Vol. 68, American Mathematical Soc.
- [15] Kardar, M., Parisi, G., Zhang, Y.-C., 1986. Dynamic Scaling of Growing Interfaces. *Physical Review Letters* 56, 889–892. <https://doi.org/10.1103/PhysRevLett.56.889>
- [16] Corwin, I., 2012. The Kardar–Parisi–Zhang equation and universality class. *Random Matrices: Theory Appl.* 01, 1130001. <https://doi.org/10.1142/S2010326311300014>
- [17] Araújo, N., Grassberger, P., Kahng, B., Schrenk, K.J., Ziff, R.M., 2014. Recent advances and open challenges in percolation. *Eur. Phys. J. Spec. Top.* 223, 2307–2321. <https://doi.org/10.1140/epjst/e2014-02266-y>
- [18] Hinrichsen, H., 2000. Non-equilibrium critical phenomena and phase transitions into absorbing states. *Advances in physics*, 49(7), pp.815-958.
- [19] Kumar, A., Dhar, D., 2020. Improved Upper Bounds on the Asymptotic Growth Velocity of Eden Clusters. *J Stat Phys* 180, 710–720. <https://doi.org/10.1007/s10955-020-02498-z>
- [20] Williams, T., Bjercknes, R., 1972. Stochastic model for abnormal clone spread through epithelial basal layer. *Nature* 236, 19–21.
- [21] Wang, Z., Bauch, C.T., Bhattacharyya, S., d’Onofrio, A., Manfredi, P., Perc, M., Perra, N., Salathé, M., Zhao, D., 2016. Statistical physics of vaccination. *Physics Reports, Statistical physics of vaccination* 664, 1–113. <https://doi.org/10.1016/j.physrep.2016.10.006>
- [22] Das, A., Dhar, A., Goyal, S., Kundu, A., 2020. Covid-19: analysis of a modified SEIR model, a comparison of different intervention strategies and projections for India. arXiv:2005.11511 [physics, q-bio].
- [23] Kordzakhia, G., 2005. The Escape Model on a Homogeneous Tree. *Electron. Commun. Probab.* 10, 113–124. <https://doi.org/10.1214/ECP.v10-1140>
- [24] Bordenave, C., 2014. Extinction probability and total progeny of predator-prey dynamics on infinite trees. *Electron. J. Probab.* 19. <https://doi.org/10.1214/EJP.v19-2361>
- [25] Tang, S., Kordzakhia, G., Lalley, S.P., 2018. Phase Transition for the Chase-Escape Model on 2D Lattices. arXiv:1807.08387 [cond-mat, q-bio].
- [26] Kesten, H., 1980. The critical probability of bond percolation on the square lattice equals 1/2. *Commun.Math. Phys.* 74, 41–59. <https://doi.org/10.1007/BF01197577>
- [27] Durrett, R., Junge, M., Tang, S., 2020. Coexistence in chase-escape. *Electron. Commun. Probab.* 25. <https://doi.org/10.1214/20-ECP302>
- [28] Owen, M.R., Lewis, M.A., 2001. How Predation can Slow, Stop or Reverse a Prey Invasion. *Bulletin of Mathematical Biology* 63, 655–684. <https://doi.org/10.1006/bulm.2001.0239>
- [29] Beckman, E., Cook, K., Eikmeier, N., Hernandez-Torres, S., Junge, M., 2020. Chase-escape with death on trees. arXiv:1909.01722 [math].
- [30] Hinsen, A., Jahnel, B., Cali, E., Wary, J.-P., 2020. Phase transitions for chase-escape models on Poisson–Gilbert graphs. *Electron. Commun. Probab.* 25. <https://doi.org/10.1214/20-ECP306>
- [31] Tomé, T., Ziff, R.M., 2010. Critical behavior of the susceptible-infected-recovered model on a square lattice. *Phys. Rev. E* 82, 051921. <https://doi.org/10.1103/PhysRevE.82.051921>
- [32] Alm, S.E., Deijfen, M., 2015. First Passage Percolation on \mathbb{Z}^2 : A Simulation Study. *J Stat Phys* 161, 657–678. <https://doi.org/10.1007/s10955-015-1356-0>
- [33] Reis, Fabio D. A. Aarao. (2003). Depinning transitions in interface growth models. *Brazilian Journal of Physics*, 33(3), 501 -513.
- [34] Derrida, B., Retaux, M. The Depinning Transition in Presence of Disorder: A Toy Model. *J Stat Phys* 156, 268–290 (2014)